

Valproic Acid Decreases the Nuclear Localization of MDT-28, the Nematode Orthologue of MED28

(Mediator complex / valproic acid / nuclear localization / MDT-28 / MED28)

M. KOSTROUCHOVÁ^{1,2,*}, V. KOSTROUCHOVÁ¹, P. YILMA¹, A. BENDA³,
V. MANDYS², M. KOSTROUCHOVÁ^{1,‡}

¹Biocev, First Faculty of Medicine, Charles University, Prague, Czech Republic

²Department of Pathology, Third Faculty of Medicine, Charles University, Prague, Czech Republic

³Imaging Methods Core Facility, Biocev, Faculty of Science, Charles University, Prague, Czech Republic

Abstract. Mediator is a multiprotein complex that connects regulation mediated by transcription factors with RNA polymerase II transcriptional machinery and integrates signals from the cell regulatory cascades with gene expression. One of the Mediator subunits, Mediator complex subunit 28 (MED28), has a dual nuclear and cytoplasmic localization and function. In the nucleus, MED28 functions as part of Mediator and in the cytoplasm, it interacts with cytoskeletal proteins and is part of the regulatory cascades including that of Grb2. MED28 thus has the potential to bring cytoplasmic regulatory interactions towards the centre of gene expression regulation. In this study, we identified MDT-28, the nema-

tode orthologue of MED28, as a likely target of lysine acetylation using bioinformatic prediction of post-translational modifications. Lysine acetylation was experimentally confirmed using anti-acetyl lysine antibody on immunoprecipitated GFP::MDT-28 expressed in synchronized *C. elegans*. Valproic acid (VPA), a known inhibitor of lysine deacetylases, enhanced the lysine acetylation of GFP::MDT-28. At the subcellular level, VPA decreased the nuclear localization of GFP::MDT-28 detected by fluorescence-lifetime imaging microscopy (FLIM). This indicates that the nuclear pool of MDT-28 is regulated by a mechanism sensitive to VPA and provides an indirect support for a variable relative proportion of MED28 orthologues with other Mediator subunits.

Received March 8, 2018. Accepted April 17, 2018.

This work was supported by the European Regional Development Fund “BIOCEV – Biotechnology and Biomedicine Centre of the Academy of Sciences and Charles University in Vestec” (CZ.1.05/1.1.00/02.0109) and the LQ1604 National Sustainability Program II (Project BIOCEV-FAR) and the project Biocev (CZ.1.05/1.1.00/02.0109) from the Ministry of Education, Youth and Sports of the Czech Republic; PROGRES Q26/LF1 and PROGRES Q28 “Oncology” from Charles University in Prague; grant SVV 260377/2017 from Charles University in Prague. The imaging was done at the Imaging Methods Core Facility at Biocev, Faculty of Science, Charles University, supported by the Czech-BioImaging large RI project (LM2015062 funded by MEYS CR). AB acknowledges the support by the MEYS CR (CZ.02.1.01/0.0/0.0/16 013/0001775 Czech-Bioimaging).

*Corresponding author: Markéta Kostrouchová, Biocev, First Faculty of Medicine, Charles University, Prague, Průmyslová 595, 252 42 Vestec, Czech Republic. Phone: (+420) 325 873 017; e-mail: marketa.kostrouchova@lf1.cuni.cz

Abbreviations: FLIM – fluorescence-lifetime imaging microscopy, MDT-28 – *C. elegans* orthologue of MED28, MED28 – Mediator complex subunit 28, NGM – nematode growth medium, PAIL – prediction of acetylation on internal lysines, RT – room temperature, TFs – transcription factors, VPA – valproic acid.

Introduction

Cell- and tissue-specific regulation of gene expression depends on transcription factors (TFs) (Reinke et al., 2013) and transcription cofactors that are expressed in a cell- and tissue-specific way (e.g. as exemplified on the mineralocorticoid receptor-dependent gene expression (Fuller et al., 2017)). TFs interact with RNA polymerase II (Pol II) basal transcriptional machinery through interaction with a multiprotein complex called Mediator complex or Mediator (Poss et al., 2013; Grants et al., 2015).

The overall structure of the Mediator complex can be divided into four modules named head, middle, tail, and the CDK8 module (Yin and Wang, 2014). Displacement of the CDK8 module forms a more transcriptionally active Mediator (Tsai et al., 2013).

The modules of Mediator consist of approximately 26 subunits in mammals, 29 subunits in *Caenorhabditis elegans* and 21 subunits in *Sacharomyces cerevisiae* (Allen and Taatjes, 2015; Grants et al., 2015). The subunit composition, arrangement and localization in the complex as well as the conformational shape of Mediator can be variable (Poss et al., 2013; Allen and Taatjes, 2015). Quantitative proteomic analysis identified under- or over-

representation of selected subunits in several human cell lines, yeast cultures and in numerous cancers (Kulak et al., 2014; Allen and Taatjes, 2015; Syring et al., 2016).

While orthologues of approximately 18 subunits can be identified both in yeast and Metazoa, some Mediator subunits are found only in yeast or only in higher metazoans. Mediator subunits that are found only in Metazoa include Med23, Med25, Med26, Med28, and Med30 (Harper and Taatjes, 2017). Mediator complex subunit 28 (MED28) is especially interesting because it not only has a nuclear, but also a cytoplasmic localization and function. In some cells and tissues MED28 is detected by specific antibodies predominantly in cytoplasmic territories, while in other cell types and tissue cultures it is detected predominantly in the nuclei, as can be seen from the data available in the Human Protein Atlas (<https://www.proteinatlas.org/>, access on January 23, 2018) (Uhlen et al., 2005, 2015, 2017; Thul et al., 2017). This protein was originally identified as a gene expressed in endothelial cells and named EG-1 (Endothelial-derived Gene-1) (Liu et al., 2002), but was later shown to be part of the Mediator complex and renamed MED28 (Sato et al., 2004; Beyer et al., 2007). MED28 (a.k.a. Magicin) also interacts with Growth factor receptor-bound protein 2 (Grb2) and Merlin and membrane-cytoskeleton scaffolding proteins at the plasma membrane (Wiederhold et al., 2004; McClatchey and Giovannini, 2005; McClatchey and Fehon, 2009) and was shown to associate with several Src-family kinases and to be their phosphorylation target (Lee et al., 2006). Overexpression of MED28 inhibits differentiation of smooth muscle cells in cell culture (Wiederhold et al., 2004).

In *C. elegans* the MED28 orthologue, MDT-28 (edited in the form expressing GFP/green fluorescent protein tagged at its N-terminus), also has a dual nuclear and cytoplasmic localization, suggesting that the capacity of transmitting cytoplasmic signals towards regulation of gene expression is evolutionarily conserved (Kostrouchová et al., 2017).

In this study we attempted to further characterize MDT-28. Bioinformatic analysis of the protein primary sequence of MDT-28 indicated that MDT-28 as well as numerous other MED28 orthologues from various phyla are likely targets of lysine acetylation. This hypothesis was supported by a positive signal of immunoprecipitated GFP::MDT-28 expressed in *C. elegans* with CRISPR/Cas-9-edited *mdt-28* that was augmented by treatment with valproic acid (VPA), a known inhibitor of lysine deacetylases. At the subcellular level, VPA treatment decreases the nuclear localization of GFP::MDT-28. The results show that the nuclear localization of MDT-28 is regulated by a mechanism sensitive to VPA, most likely by acetylation of lysines present in MDT-28 itself or in nuclear proteins interacting with MDT-28.

Material and Methods

Bioinformatics and identification of lysine acetylation

For prediction of lysine acetylation, the online predictor for protein acetylation PAIL (prediction of acetylation on internal lysines) was used (available at <http://pail.biocuckoo.org/online.php>) with threshold accuracy set at 85.13 %, 87.97 % and 89.21 % for low, medium and high thresholds, respectively (Li et al., 2006). Sequences of experimentally proven MDT-28 or of predicted orthologues were retrieved from GenBank (<https://www.ncbi.nlm.nih.gov/genbank/>) (Benson et al., 2013, 2017) (Table 1).

Strains, transgenic lines and genome editing

The *C. elegans* strain KV4 was used in which the gene for MDT-28 (F28F8.5b) was modified to *gfp::mdt-28* in its normal genomic position ($P_{F28F8.5}(V:15573749)::gfp::mdt-28$) on both alleles. The expressed GFP::MDT-28 was used for pull-down and fluorescence microscopy experiments. For details see Kostrouchová et al. (2017). A strain expressing GFP only from extrachromosomal

Table 1. Predicted acetylation sites of MED28 orthologues

Species	ID	Position	Peptide	HAT	Score	Cutoff	Stringency
<i>C. elegans</i>	H9G301.1 mdt-28	198	EAHPNAGKHFTT***	CREBBP	1.548	1.348	M
<i>T. spiralis</i>	tr E5RZQ1 E5RZQ1_TRISP	163	KLTCSDWKIALES**	CREBBP	1.355	1.348	M
<i>W. bancrofti</i>	EJW84794.1	160	LSDLGAEKNSQGF*	CREBBP	1.851	1.785	H
<i>D. melanogaster</i>	Q9VBQ9.1	189	ISRQMPPK*****	CREBBP	2.161	1.785	H
<i>H. sapiens</i>	Q9H204.1	176	ANIPAPLKPT*****	CREBBP	2.165	1.785	H
<i>M. musculus</i>	Q920D3.2	176	ANIPAPLKQT*****	CREBBP	2.532	1.785	H
<i>T. rubripes</i>	XP_003972471.1	178	NLPPAPLKPS*****	CREBBP	2.698	1.785	H
<i>X. tropicalis</i>	AAI55039.1 med28	167	ANIPAPMKPT*****	CREBBP	2.165	1.785	H
<i>C. intestinalis</i>	XP_002124297.1	141	GAGSQQMKK*****	CREBBP	3.391	1.785	H
<i>C. intestinalis</i>	XP_002124297.1 28-like	142	AGSQQMKK*****	CREBBP	3.048	1.785	H
<i>T. adhaerens</i>	XM_002117398.1	105	QQDLTKWKE*****	CREBBP	2.992	1.785	H

arrays under the regulation of the promoter of *nhr-180* (nuclear hormone receptor 180) was used as control for GFP::MDT28 pull-down experiments.

Valproic acid (VPA) treatment

These experiments were done on either nematode growth medium (NGM) plates or in liquid cultures containing a final concentration of 0 or 1 mM or 5 mM valproate (valproic acid sodium salt, Sigma-Aldrich, St. Louis, MO). OP50 bacteria also containing valproate at a final concentration of 0 or 1 mM or 5 mM covered the entire area of the respective plates. Synchronization of animals of the *C. elegans* strain KV4 was done using the bleach method overnight. The next day the L1 larvae were incubated with one of the three concentrations of valproate for 4 h or 24 h at room temperature (RT, 22 °C).

For FLIM experiments, control and VPA-treated nematodes were then placed in a 10 µl drop of PBS 1x on a glass microscopic slide (Waldemar Knittel Glasbearbeitungs-GmbH, Braunschweig, Germany) containing a layer of 2% agarose, immobilized with 1 mM levamisole (Sigma-Aldrich) and covered with a cover glass of thickness 0.13–0.17 mm with a refraction index of 1.523 (Hirschmann Laborgeräte GmbH & Co, Eberstadt, Germany).

For GFP-Trap experiments, after incubation with or without valproate the nematodes were washed with water followed by PBS 1x from plates, rocked for 10 min at room temperature, and pelleted 2 times by centrifugation at 250 × *g* for 3 min at 4 °C in 13 ml tubes, then in Eppendorf tubes (2 min at 330 × *g*, 4 °C). The worm pellets were immediately resuspended in 320 µl of ice-cold lysis buffer (10 mM Tris/Cl pH 7.5, 150 mM NaCl, 0.5 mM EDTA, 0.5% NP-40) with added protease inhibitors (Halt Protease and Phosphatase Inhibitor Cocktail (100x), Thermo Fisher Scientific, Waltham, MA) and vortexed with interruptions on ice for 10 min, followed by sonication (3 × 10 s). The lysed samples were spun down by centrifugation at 19,000 × *g* for 5 min at 4 °C and the supernatant was stored at –80 °C before performing GFP-Trap experiments.

GFP-Trap and proteomic analysis of MDT-28 acetylation

GFP-Trap experiments were done using GFP-Trap[®] MA (ChromoTek Inc., Hauppauge, NY) according to manufacturer's instructions with modifications. Experiments were done at constant excess of active beads (10 µl of bead slurry) that were incubated with the same amount of one of the three types of lysed samples obtained from animals treated with vehicle (deionized sterile water) or 1 mM or 5 mM VPA for 1 h at 4 °C. Beads with bound GFP or GFP::MDT-28 were magnetically separated and washed three times with Dilution/Wash buffer (10 mM Tris/Cl pH 7.5, 150 mM NaCl, 0.5 mM EDTA). The purified beads were then resuspended in 70 µl of 2× Tris-glycin SDS sample buffer (Thermo Fisher Scientific) and 2 µl of β-mercaptoethanol.

To dissociate immunocomplexes from the beads, 95 °C heat was applied for 10 min followed by centrifugation at around 13,000 × *g* for 5 min at RT, and samples were stored at 4 °C.

For Western blotting, 10 µl or 20 µl of each supernatant was loaded on two SDS-gels, separated by electrophoresis and then blotted onto two BioTrace[™] PVDF transfer membranes using the Mini-PROTEAN Tetra Cell (Bio-Rad, Hercules, CA). Blocking was done in either 0.3 % (for detection of acetylated lysine) or 5 % (for detection of GFP) non-fat milk in T-PBS for 30 min at RT. Incubation with primary antibodies was done with shaking overnight at 4 °C. Primary antibodies used were mouse acetyl-lysine monoclonal antibody 1C6 (at a dilution of 1 : 1000) (Abcam, Cambridge, MA) and mouse GFP antibody B-2 (at a dilution of 1 : 222) (sc-9996, Santa Cruz Biotechnology, Santa Cruz, CA). Secondary antibody used was goat anti-mouse antibody (H+L)-HRP conjugate (1 : 10,000) (Bio-Rad).

Fluorescence-lifetime imaging microscopy (FLIM)

FLIM acquisition was done as described (Kostrouchova et al., 2017). Briefly, the single photon counting signal from the internal hybrid detectors in Leica TC SP8 SMD FLIM (Leica, Wetzlar, Germany), acquired during confocal acquisitions, was simultaneously processed by HydraHarp400 TCSPC electronics (PicoQuant, Berlin, Germany). General data structure, the demo program description and user instructions are accessible at https://github.com/PicoQuant/PicoQuant-Time-Tagged-File-Format-Demos/blob/master/PTU/Matlab/Read_PTU.m. We used our own implementation of TTTR data analysis, written in LabVIEW, which allows proper handling of the bidirectional harmonic scan with line accumulation and/or sequential excitation. The emission signal upon 488 nm excitation was spectrally split into two hybrid detectors with similar intensity at each of them to lower the detector saturation at bright pixels. The signal from both time synchronized channels was added up. The false colour scale (1 to 3 ns) is based on the average photon arrival time.

Densitometric analysis of FLIM images

FLIM data of the *C. elegans* KV4 strain were recorded at identical settings in one microscopic session and exported as false colour scale images in TIFF format in two assembled files for 4 h and 24 h incubation with or without VPA. Experiments after 4 h incubation included controls (exposed to vehicle only) and animals exposed to 1 mM or 5 mM VPA. Experiments after 24 h incubation included controls and animals treated with 1 mM VPA. To remove the contribution of autofluorescence from the quantification of overall densities, the GFP signal amplitude in each pixel was estimated from the average arrival time of photons in that pixel, assuming a two-component model consisting of GFP and the autofluorescence signal. The amplitude of the GFP signal was encoded as the red channel in the exported false

colour images. Exported TIFF images were analysed using the ImageJ program. The images were split to individual channels and all clearly defined intestinal nuclei in the red channel recordings were densitometrically analysed (using the rectangle selection tool). The rectangles were set as the minimum possible rectangles that could be drawn around the nuclei, touching the nuclei on four sides.

Results

Bioinformatic analyses of MED28 orthologues reveal a high probability of lysine acetylation

The 202 amino acid sequence of MDT-28/F28F8.5b (WormBase ID: WP:CE47319, www.wormbase.org/species/c_elegans/protein/WP:CE47319#06-10K) contains four lysines: K107, K120, K128 and K198. For the prediction of possible lysine acetylation we used the online bioinformatic tool PAIL (<http://bdmpail.biocuckoo.org>). Under medium stringency settings all four lysines in the primary amino acid sequence were identified as targets of acetylation. Under high stringency settings, lysines 128 and 198 were identified with a score of 1.20 and 2.13, respectively against a threshold of 0.5.

We then used the GPS-PAIL program (<http://pail.biocuckoo.org/online.php>) for the prediction of substrates and sites of seven histone acetyltransferases that identified K198 as the likely target of CREB-binding protein (CBP, CREBBP), also under medium stringency settings (with a score of 1.548 at 1.348 cutoff) (Table 1). The same prediction tool identified a high probability of lysine acetylation in all selected protein sequences of the known Mediator subunit 28 orthologues across the animal kingdom (Table 1).

The sequence analysis for targets of defined acetyltransferases (NP_079481.2) identified the most C-terminal lysine (K176) of human MED28 as the likely target of CBP-mediated acetylation (with the score of 2.165) (Table 1). In both the human MED28 and the *C. elegans* orthologue, the lysines recognized as the likely targets of CBP-dependent acetylation are the most C-terminal lysines located in the regions that are not classified by homology searches as conserved. These C-terminally positioned lysines are conserved within the metazoan classes. While in nematodes the lysines identified as CBP targets are the 5th, 6th or 7th amino acid from the C-terminal end in *C. elegans*, *T. spiralis* and *W. bancrofti*, respectively, in *Drosophila* it is the last C-terminal amino acid, in vertebrates it is the 3rd terminal amino acid, the second to last or last in *Ciona intestinalis*, and in the sequence retrieved from the *T. adhaerens* genome using the Blast program as the closest sequence to human MED28, there is a lysine recognized as a likely CBP target also in the second to last amino acid (Table 1). In several insect species, the prediction of acetylated lysines is not found in the most C-terminal part of predicted proteins, but several other lysines are identified as likely targets of acetylation under high stringency set-

tings (e.g., in XP_011140830.1, the predicted mediator of RNA polymerase II transcription subunit 28 isoform X2 of *Harpegnathos saltator*). The prediction was also done using the GPS-PAIL computer program (<http://pail.biocuckoo.org/online.php>).

C. elegans GFP::MDT-28 is dynamically acetylated

To test whether or not MDT-28 is acetylated, we used the *C. elegans* strain KV4 expressing GFP::MDT-28 from both edited alleles containing the edited gene *gfp::mdt-28*. The GFP::MDT-28 fusion protein was immunoprecipitated using the GFP-Trap system (in excess of beads with single-chain anti-GFP antibody) from synchronized animals, and acetylated lysines were detected on Western blot using an anti-acetylated lysine monoclonal antibody. The anti-acetylated lysine antibody yielded a positive signal on the fusion protein but not on GFP alone, supporting the presence of acetylated lysines in MDT-28. The signal obtained with the anti-acetyl lysine antibody was considerably weaker compared to that obtained with the anti-GFP antibody. We therefore treated synchronized cultures of *C. elegans* larvae with VPA, a known inhibitor of histone deacetylases. In keeping with the prediction, VPA increased the signal detected by anti-lysine antibody more than the expression of GFP::MDT-28 detected by the anti-GFP antibody (Fig. 1).

Valproic acid decreases the intranuclear localization of GFP::MDT-28

To visualize GFP::MDT-28 localization we used FLIM, which is able to detect and resolve from the autofluorescence background the weak signal of GFP::MDT-28 expressed from its two edited alleles, and we compared the basal state of its expression with that after the treatment with 1 mM and 5 mM VPA. While under basal conditions GFP::MDT-28 was localized predominantly in the nuclei with a prominent dotted pattern, treatment with 1 mM and 5 mM VPA for 4 h decreased the gross nuclear expression of GFP::MDT-28 and its dotted character (Fig. 2). Densitometric analysis of the values exported in the red channel confirmed the overall decrease of GFP::MDT-28 nuclear presence in *C. elegans* incubated with 1 and 5 mM VPA (Fig. 3). This effect of VPA was even more apparent in animals treated with VPA for 24 h (Fig. 4). The strong FLIM signal visible in the nuclei in a dotted pattern decreased after 24 h treatment with 1 mM VPA. Densitometric analysis of the values exported in the red channel taken after 24 h also confirmed a strong decrease of GFP::MDT-28 intranuclear localization after the treatment with VPA (Fig. 5).

Discussion

While most Mediator complex subunits have characteristics of predominantly or exclusively nuclear proteins,

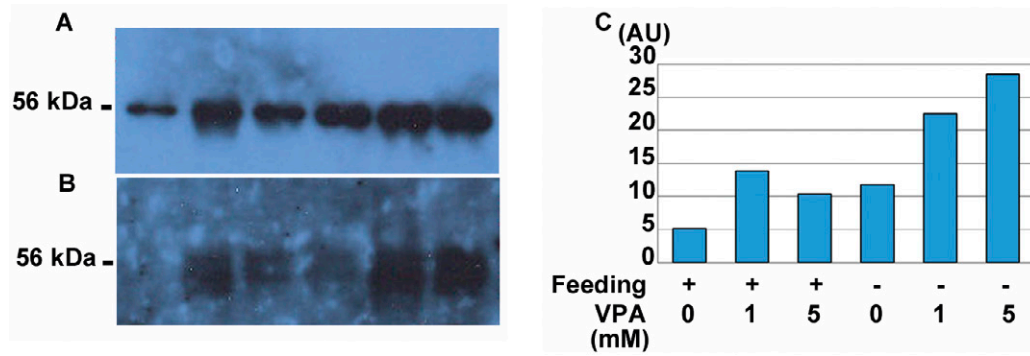


Fig. 1. Detection of acetylated lysines of MDT-28 in fed or starved synchronized L1 larvae and incubated for 4 h with 1 mM VPA or 5 mM VPA or without VPA. Panels **A** and **B** show Western blots of immunoprecipitated GFP::MDT-28 pulled-down by the GFP-Trap system and probed with anti-GFP antibody (panel **A**) and anti-acetylated lysine antibody (panel **B**). Panel **C** shows the densitometric analysis of the levels of immunodetected lysine-acetylated GFP::MDT-28 shown in panel **B** normalized for the expression of GFP::MDT-28 with subtracted background staining and adjusted for loading volumes (10 μ l in the first three lanes in panel **A** representing fed cultures and 20 μ l in all the remaining lanes). The Western blot and its analysis is one of two independent experiments with similar results. The densitometric analysis indicates elevated lysine acetylation in larvae cultured in the presence of VPA. The background staining observed in Western blots with anti-acetyl lysine antibody reflects the necessity for long time exposures for the visualization of acetylated lysine, likely indicating that the acetylated GFP::MDT-28 constitutes a minor proportion of the total GFP::MDT-28. The animals were synchronized by starvation after hatching and incubated for 4 hours with or without addition of bacterial food.

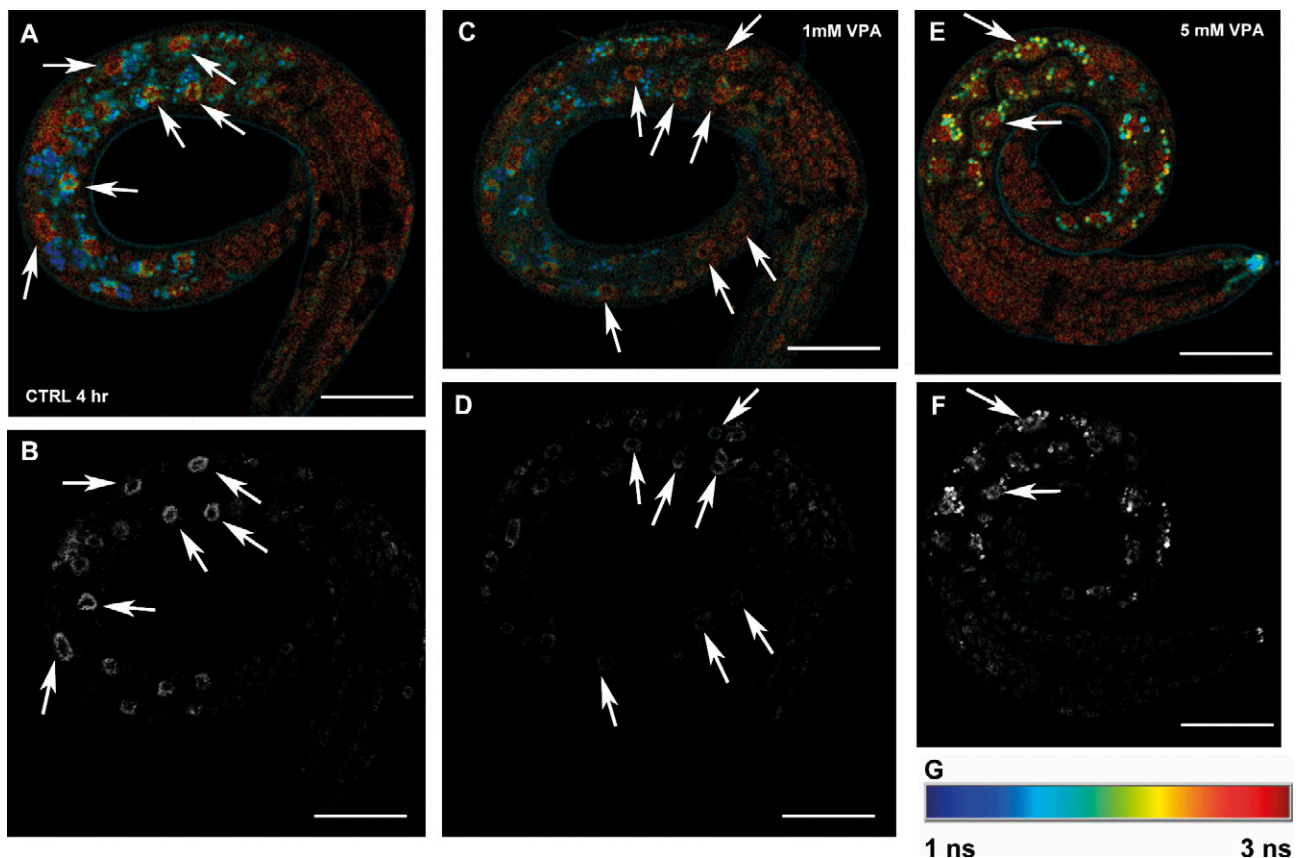


Fig. 2. The effect of short-term (4 h) exposure to VPA on the intracellular distribution of GFP::MDT-28 in synchronized *C. elegans* L1 larvae. Panels **A** and **B** show a control L1 larva (no VPA), panels **C** and **D** an L1 larva after treatment with 1 mM VPA, and panels **E** and **F** a larva treated with 5 mM VPA. Panels **A**, **C** and **E** show computed false colour FLIM images. The reference table of average photon arrival time in FLIM images is shown in panel **G**. Panels **B**, **D** and **F** are the red channel images corresponding to the signal from GFP only and show a visible decrease of GFP signal in the larvae incubated with 1 and 5 mM VPA. Bars represent 25 μ m.

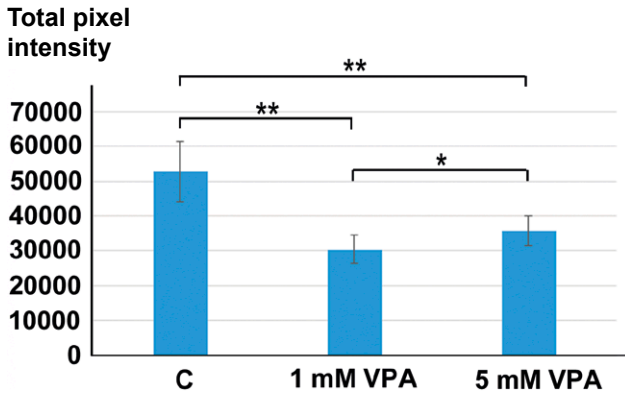


Fig. 3. Densitometric analysis of GFP::MDT-28 FLIM signal in the nuclei of enterocytes of a control larva and larvae incubated with 1 mM and 5 mM VPA for 4 h. The GFP only signal, exported as red channel data obtained for individual nuclei, was analysed densitometrically using the ImageJ program. All clearly defined enterocyte nuclei (N = 35, N = 29 and N = 22, for control nuclei, nuclei of a larva incubated with 1 mM VPA and nuclei of a larva incubated with 5 mM VPA, respectively) were analysed. The values represent total pixel intensity. The P values of the *t*-test of paired sets, for which the null hypothesis is considered as no statistical difference between the two evaluated sets, are as follows: $P = 1.61 \times 10^{-8}$ for control versus 1 mM VPA, $P = 3.67096 \times 10^{-6}$ for control versus 5 mM VPA, $P = 0.031745$ for 1 mM VPA versus 5 mM VPA. The results show a statistically significant decrease of GFP::MDT-28 in the nuclei of enterocytes treated with 1 and 5 mM VPA versus control nuclei ($* < 0.05$, $** < 0.00001$).

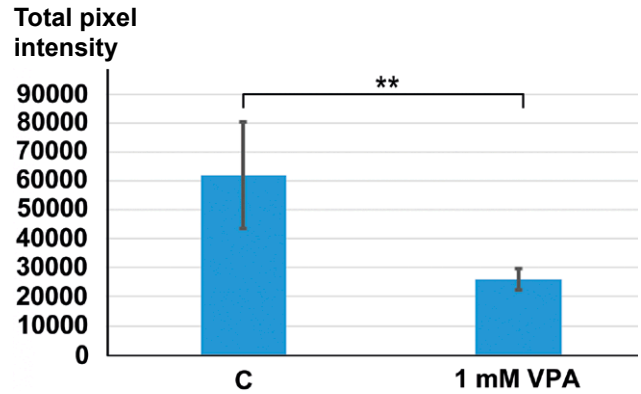


Fig. 5. Densitometric analysis of GFP::MDT-28 FLIM signal in clearly defined enterocyte nuclei of a control larva and a larva incubated with 1 mM VPA for 24 h. The values represent total pixel intensity. The P value of the *t*-test, for which the null hypothesis is considered as no statistical difference between the two evaluated sets, is $P = 4.566 \times 10^{-5}$. The result shows a significant decrease of the GFP::MDT-28 signal in the nuclei of enterocytes after 1 mM VPA treatment ($** < 0.0001$). N = 26 for control nuclei and N = 20 for nuclei of a larva treated with 1 mM VPA for 24 h.

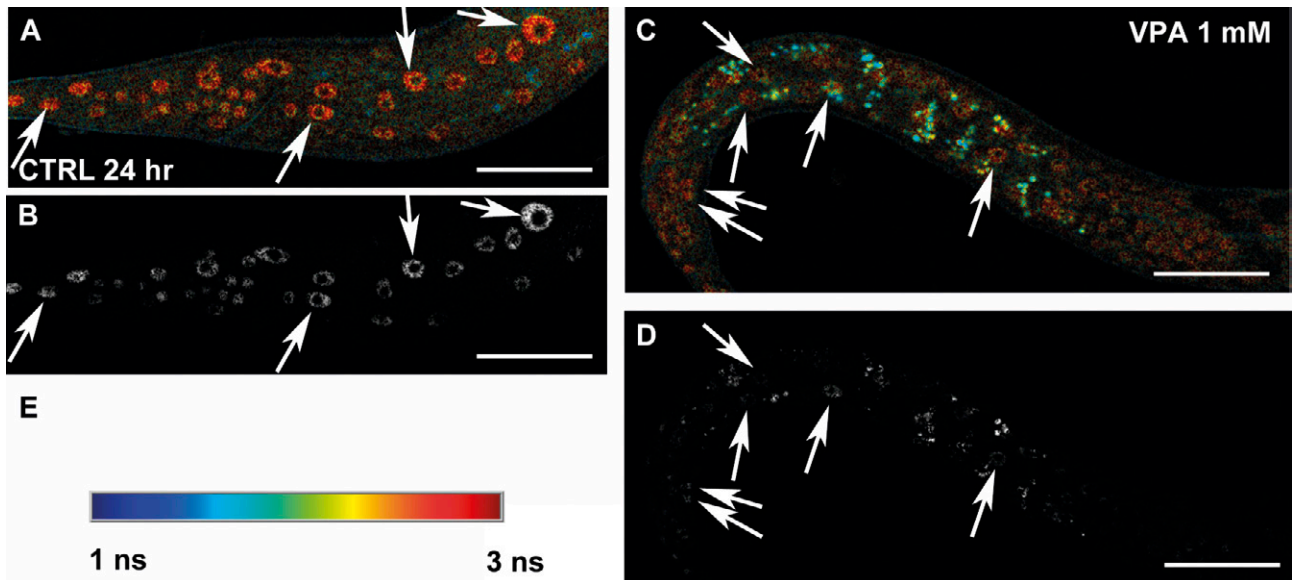


Fig. 4. The effect of 24-h exposure of synchronized *C. elegans* starting from the L1 stage to valproic acid on the intracellular distribution of GFP::MDT-28. Panels **A** and **B** show a control larva and panels **C** and **D** a larva incubated with 1 mM VPA. Panels **A** and **C** show computed false colour FLIM images of the overall signal. The reference table of average photon arrival time in FLIM images is shown in panel **E**. Panels **B** and **D**, derived from the red channel of false colour FLIM images, display intracellular distribution of GFP::MDT-28 and show a visible decrease of the GFP signal in the larva incubated with 1 mM VPA. Bars represent 25 μm.

MED28 has a proven nuclear as well as cytoplasmic localization and functions as a cytoskeleton-associated protein interacting with Grb2 (Wiederhold et al., 2004) and a Mediator subunit in the nucleus (Sato et al., 2004; Beyer et al., 2007). This suggests the possibility that MED28 may bring cytoplasmic regulatory signals towards the regulation of gene expression when its interacting proteins co-localize with MED28 in the nucleus as well. In such a case, translocations of MED28 and its interacting proteins may be part of the regulatory circuits and may have the potential of mediating cell structural signals towards the regulation of gene expression.

In this work we attempted to further characterize MDT-28 that we previously identified in the *C. elegans* genome (Kostrouchova et al., 2017). Analysis of the MDT-28 sequence using bioinformatic tools identified MDT-28 along with several other MED28 orthologues as likely targets of lysine acetylation. To test this possibility, we used the GFP-Trap system for immunoprecipitation of GFP::MDT-28 expressed in a transgenic line containing the edited *mdt-28* gene, probed it with a commercially available antibody raised against peptides containing acetylated lysines and confirmed the presence of acetylated lysines in GFP::MDT-28. Treatment with VPA, a known inhibitor of histone deacetylases, increased the proportion of acetylated GFP::MDT-28, indicating that the acetylation of GFP::MDT-28 may be dynamic and is subjected to deacetylation by HDACs sensitive to VPA. We then wanted to know whether exposure of nematodes to VPA affects GFP::MDT-28 *in vivo*. In line with this possibility we detected changes of GFP::MDT-28 intranuclear localization visualized as decreased presence of GFP::MDT-28 in the nuclei and a change of the signal pattern. While under control conditions GFP::MDT-28 was detected in a punctuate intranuclear pattern, treatment with VPA decreased the presence in the punctuate centres as well as the overall sum of the GFP signal in the nuclei.

Studies focused on the localization and function(s) of MED28 identified separately its cytoplasmic and nuclear localizations, but rarely reported both localizations. Wiederhold et al. (2004) recognized MED28 (Magicin) cytoplasmic function and interaction with cytoplasmic Grb2 and NF2 tumour-associated protein Merlin and observed MED28 in the cytoplasm associated with actin-containing cytoskeleton. In contrast, studies that identified the nuclear function of MED28 as a component of the Mediator complex proved its localization in the nuclear fractions (Paoletti et al., 2006; Beyer et al., 2007). Our previous work exploited transgenic lines of *C. elegans* carrying MDT-28 fused with GFP under the regulation of the endogenous internal promoter (expressed as MDT-28::GFP from extrachromosomal arrays) and *C. elegans* lines with edited *mdt-28* gene (expressing GFP::MDT-28 from its genomic locus). Both experimental settings proved the dual nuclear and cytoplasmic localization of MDT-28 (Kostrouchova et al., 2017).

Additional data concerning the nuclear and cytoplasmic localization of MED-28 can be found in The Hu-

man Protein Atlas. Interestingly, the two antibodies (HPA035900 and HPA035901, produced by Sigma-Aldrich) that were used identified MED28 only rarely (presumably) in the same localization and in the same cell types. The protein species recognized by the two antibodies have sizes of approximately 21, 29, 42, 47 and 63 kDa in the case of HPA035900 and 32, 36 kDa in the case of HPA 035901 (the data was accessed in The Human Protein Atlas on Jan 7, 2018) (Uhlen et al., 2005, 2015, 2017; Thul et al. 2017). Another antibody, MABC1143, anti-MED28 antibody, clone 7E1 available from Merck (Merck & Co, Kenilworth, NJ) recognizes a protein with an approximate size of 20 kDa and gives clear positive signal in both the nuclei and cytoplasm in the mouse blastocyst (Li et al., 2015). These results may reflect extensive posttranslational modification of MDT-28 and selective affinities of antibodies binding to different epitopes on the MDT-28 molecule.

In our experiments, edited MDT-28 (GFP::MDT-28) was expressed as protein species with two close sizes in the expected size range (approximately 56 kDa: GFP 29.6 kDa and MDT-28 22.5 kDa, plus the linker) detected using anti-GFP antibody. The two sizes are likely to reflect posttranslational modifications of MDT-28. Immunodetection of acetylated lysines in GFP::MDT-28 immunoprecipitated by anti-GFP single-chain antibody (using the GFP Trap system) is relatively weak compared to detection obtained by anti-GFP antibody (that differed from the single-chain antibody used in the GFP Trap system). It is possible that the affinity of the antibody raised against acetylated lysines in human H3 histone is relatively low for interaction with acetylated lysines in *C. elegans* MDT-28, but it cannot be ruled out that the proportion of MDT-28 with acetylated lysines may be small and the acetylation of lysines in MDT-28 may be transient and quickly removed. Bioinformatic and experimental studies of Mediator subunits (Nagulapalli et al., 2016) indicated that intrinsically disordered regions and the likelihood for posttranslational modifications are partially conserved, but show tendency to become more complex during evolution in both protein-protein interactions and their modulation by posttranslational modifications. Bioinformatic analysis of lysine acetylation in MDT-28 presented in this study and the presence of intrinsically disordered regions that can be detected by GlobPlot (<http://globplot.embl.de/cgiDict.py>, accessed on January 7, 2018) (Linding et al., 2003) is well in keeping with the data shown for human MED28 (Nagulapalli et al., 2016) (Fig. 6).

It is still debated whether Mediator complex subunits are in all cells in equimolar stoichiometric ratios, or may be present in different ratios in different cell types or physiological states. The observation of the decrease in the nuclear pool of MDT-28 in response to the treatment with VPA strongly supports variable representation of MDT-28 in the nuclei with ongoing tissue-specific gene expression.

Our results clearly show that MDT-28 nuclear localization is regulated by a mechanism sensitive to VPA.

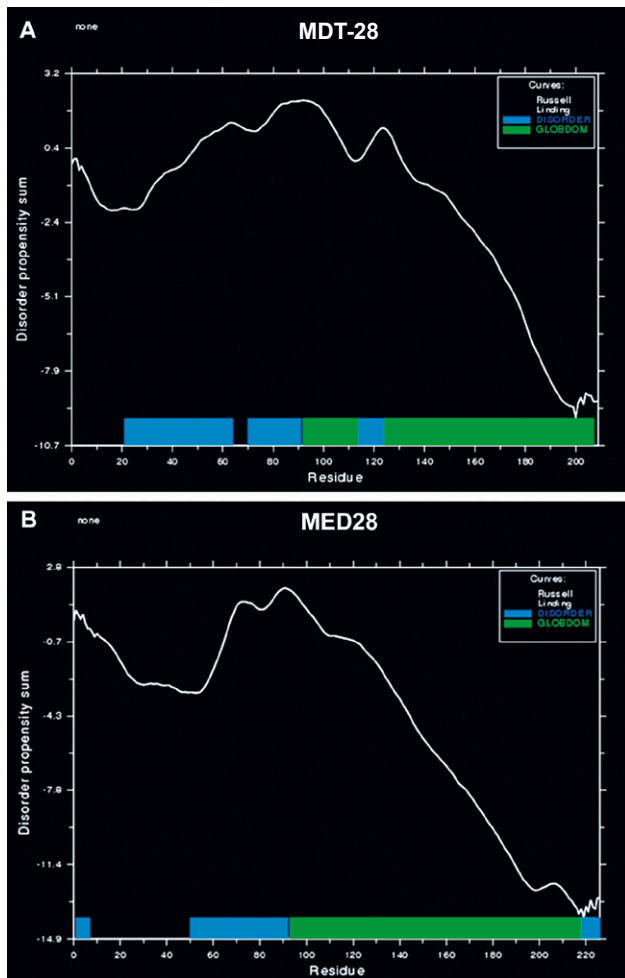


Fig. 6. Schematic representation of intrinsically disordered regions in MDT-28 (panel A) and human MED28 (panel B). This schematic representation was done using GlobPlot (<http://globplot.embl.de/cgiDict.py>). Both proteins show similar distribution of intrinsically disordered regions indicated by blue rectangles and structurally organized regions (detected as Globodomains) indicated by green rectangles. The globular domains are recognized as α structured domains in four models obtained by the SWISS-MODEL (<https://swissmodel.expasy.org/interactive/ahvMcA/models/>, accessed on February 13, 2018) based on templates MED21, RalA-binding protein 1, Apolipoprotein E, and Apolipoprotein A-1. However, high fidelity of the models cannot be expected since no closer templates are available.

VPA was shown to both increase and decrease expression of distinct sets of genes in leukaemia (Stamatopoulos et al., 2009) as well as in non-tumorous cells (Jergil et al., 2011) and was shown to be connected to elevated levels of acetylated histones (reviewed in (Kostrouchova et al., 2007)) and repeatedly reported in many studies (Fukuchi et al., 2009). Increased acetylation in the promoters of histones may well explain the elevated expression of repressed genes, but is unlikely to explain the down-regulation of sets of genes after the treatment with VPA. Our data may indirectly support the existence of

Mediator complexes with and without MED28 and the effect of VPA on the composition and function of the Mediator complex. Our results support the possibility that VPA interferes with a mechanism that is involved in the regulation of the intracellular localization of MDT-28.

Acknowledgement

The authors would like to especially thank Zdenek Kostrouch for advice. Please distinguish similar names of coauthors: *Markéta Kostrouchová, ‡ Marta Kostrouchová.

References

- Allen, B. L., Taatjes, D. J. (2015) The Mediator complex: a central integrator of transcription. *Nat. Rev. Mol. Cell Biol.* **16**, 155-166.
- Benson, D. A., Cavanaugh, M., Clark, K., Karsch-Mizrachi, I., Lipman, D. J., Ostell, J., Sayers, E. W. (2013) GenBank. *Nucleic Acids Res.* **41**, D36-42.
- Benson, D. A., Cavanaugh, M., Clark, K., Karsch-Mizrachi, I., Lipman, D. J., Ostell, J., Sayers, E. W. (2017) GenBank. *Nucleic Acids Res.* **45**, D37-D42.
- Beyer, K. S., Beauchamp, R. L., Lee, M. F., Gusella, J. F., Naar, A. M., Ramesh, V. (2007) Mediator subunit MED28 (Magicin) is a repressor of smooth muscle cell differentiation. *J. Biol. Chem.* **282**, 32152-32157.
- Fukuchi, M., Nii, T., Ishimaru, N., Minamino, A., Hara, D., Takasaki, I., Tabuchi, A., Tsuda, M. (2009) Valproic acid induces up- or down-regulation of gene expression responsible for the neuronal excitation and inhibition in rat cortical neurons through its epigenetic actions. *Neurosci. Res.* **65**, 35-43.
- Fuller, P. J., Yang, J., Young, M. J. (2017) 30 YEARS OF THE MINERALOCORTICOID RECEPTOR: Coregulators as mediators of mineralocorticoid receptor signalling diversity. *J. Endocrinol.* **234**, T23-T34.
- Grants, J. M., Goh, G. Y., Taubert, S. (2015) The Mediator complex of *Caenorhabditis elegans*: insights into the developmental and physiological roles of a conserved transcriptional coregulator. *Nucleic Acids Res.* **43**, 2442-2453.
- Harper, T. M., Taatjes, D. J. (2017) The complex structure and function of Mediator. *J. Biol. Chem.* doi: 10.1074/jbc.R117.794438
- Jergil, M., Forsberg, M., Salter, H., Stockling, K., Gustafson, A. L., Dencker, L., Stigson, M. (2011) Short-time gene expression response to valproic acid and valproic acid analogs in mouse embryonic stem cells. *Toxicol. Sci.* **121**, 328-342.
- Kostrouchova, M., Kostrouch, Z., Kostrouchova, M. (2007) Valproic acid, a molecular lead to multiple regulatory pathways. *Folia Biol. (Praha)* **53**, 37-49.
- Kostrouchova, M., Kostrouch, D., Chughtai, A. A., Kassak, F., Novotny, J. P., Kostrouchova, V., Benda, A., Krause, M. W., Saudek, V., Kostrouchova, M., Kostrouch, Z. (2017) The nematode homologue of Mediator complex subunit 28, F28F8.5, is a critical regulator of *C. elegans* development. *PeerJ.* **5**, e3390.
- Kulak, N. A., Pichler, G., Paron, I., Nagaraj, N., Mann, M. (2014) Minimal, encapsulated proteomic-sample process-

- ing applied to copy-number estimation in eukaryotic cells. *Nat. Methods* **11**, 319-324.
- Lee, M. F., Beauchamp, R. L., Beyer, K. S., Gusella, J. F., Ramesh, V. (2006) Magicin associates with the Src-family kinases and is phosphorylated upon CD3 stimulation. *Biochem. Biophys. Res. Commun.* **348**, 826-831.
- Li, A., Xue, Y., Jin, C. J., Wang, M. H., Yao, X. B. (2006) Prediction of N-ε-acetylation on internal lysines implemented in Bayesian Discriminant Method. *Biochem. Biophys. Res. Commun.* **350**, 818-824.
- Li, L., Walsh, R. M., Wagh, V., James, M. F., Beauchamp, R. L., Chang, Y. S., Gusella, J. F., Hochedlinger, K., Ramesh, V. (2015) Mediator subunit Med28 is essential for mouse peri-implantation development and pluripotency. *PLoS One* **10**, e0140192.
- Linding, R., Russell, R. B., Neduva, V., Gibson, T. J. (2003) GlobPlot: exploring protein sequences for globularity and disorder. *Nucleic Acids Res.* **31**, 3701-3708.
- Liu, C., Zhang, L., Shao, Z. M., Beatty, P., Sartippour, M., Lane, T. F., Barsky, S. H., Livingston, E., Nguyen, M. (2002) Identification of a novel endothelial-derived gene EG-1. *Biochem. Biophys. Res. Commun.* **290**, 602-612.
- McClatchey, A. I., Giovannini, M. (2005) Membrane organization and tumorigenesis – the NF2 tumor suppressor, Merlin. *Genes Dev.* **19**, 2265-2277.
- McClatchey, A. I., Fehon, R. G. (2009) Merlin and the ERM proteins – regulators of receptor distribution and signaling at the cell cortex. *Trends Cell. Biol.* **19**, 198-206.
- Nagulapalli, M., Mají, S., Dwivedi, N., Dahiya, P., Thakur, J. K. (2016) Evolution of disorder in Mediator complex and its functional relevance. *Nucleic Acids Res.* **44**, 1591-1612.
- Paoletti, A. C., Parmely, T. J., Tomomori-Sato, C., Sato, S., Zhu, D., Conaway, R. C., Conaway, J. W., Florens, L., Washburn, M. P. (2006) Quantitative proteomic analysis of distinct mammalian Mediator complexes using normalized spectral abundance factors. *Proc. Natl. Acad. Sci. USA* **103**, 18928-18933.
- Poss, Z. C., Ebmeier, C. C., Taatjes, D. J. (2013) The Mediator complex and transcription regulation. *Crit. Rev. Biochem. Mol. Biol.* **48**, 575-608.
- Reinke, V., Krause, M., Okkema, P. (2013) Transcriptional regulation of gene expression in *C. elegans*. *WormBook* 1-34.
- Sato, S., Tomomori-Sato, C., Parmely, T. J., Florens, L., Zybailov, B., Swanson, S. K., Banks, C. A., Jin, J., Cai, Y., Washburn, M. P., Conaway, J. W., Conaway, R. C. (2004) A set of consensus mammalian mediator subunits identified by multidimensional protein identification technology. *Mol. Cell* **14**, 685-691.
- Stamatopoulos, B., Meuleman, N., De Bruyn, C., Mineur, P., Martiat, P., Bron, D., Lagneaux, L. (2009) Antileukemic activity of valproic acid in chronic lymphocytic leukemia B cells defined by microarray analysis. *Leukemia* **23**, 2281-2289.
- Syring, I., Klumper, N., Offermann, A., Braun, M., Deng, M., Boehm, D., Queisser, A., von Massenhausen, A., Bragelmann, J., Vogel, W., Schmidt, D., Majores, M., Schindler, A., Kristiansen, G., Muller, S. C., Ellinger, J., Shaikhibrahim, Z., Perner, S. (2016) Comprehensive analysis of the transcriptional profile of the Mediator complex across human cancer types. *Oncotarget* **7**, 23043-23055.
- Thul, P. J., Akesson, L., Wiking, M., Mahdessian, D., Geladaki, A., Ait Blal, H., Alm, T., Asplund, A., Bjork, L., Breckels, L. M., Backstrom, A., Danielsson, F., Fagerberg, L., Fall, J., Gatto, L., Gnann, C., Hober, S., Hjelmare, M., Johansson, F., Lee, S., Lindskog, C., Mulder, J., Mulvey, C. M., Nilsson, P., Oksvold, P., Rockberg, J., Schutten, R., Schwenk, J. M., Sivertsson, A., Sjostedt, E., Skogs, M., Stadler, C., Sullivan, D. P., Tegel, H., Winsnes, C., Zhang, C., Zwahlen, M., Mardinoglu, A., Ponten, F., von Feilitzen, K., Lilley, K. S., Uhlen, M., Lundberg, E. (2017) A subcellular map of the human proteome. *Science* **356**, 10.1126/science.aal3321.
- Tsai, K. L., Sato, S., Tomomori-Sato, C., Conaway, R. C., Conaway, J. W., Asturias, F. J. (2013) A conserved Mediator-CDK8 kinase module association regulates Mediator-RNA polymerase II interaction. *Nat. Struct. Mol. Biol.* **20**, 611-619.
- Uhlen, M., Bjorling, E., Agaton, C., Szgyarto, C. A., Amini, B., Andersson, E., Andersson, A. C., Angelidou, P., Asplund, A., Asplund, C., Berglund, L., Bergstrom, K., Brumer, H., Cerjan, D., Ekstrom, M., Elobeid, A., Eriksson, C., Fagerberg, L., Falk, R., Fall, J., Forsberg, M., Bjorklund, M. G., Gumbel, K., Halimi, A., Hallin, I., Hamsten, C., Hansson, M., Hedhammar, M., Hercules, G., Kampf, C., Larsson, K., Lindskog, M., Lodewyckx, W., Lund, J., Lundberg, J., Magnusson, K., Malm, E., Nilsson, P., Odling, J., Oksvold, P., Olsson, I., Oster, E., Ottosson, J., Paavilainen, L., Persson, A., Rimini, R., Rockberg, J., Runeson, M., Sivertsson, A., Skolleremo, A., Steen, J., Stenvall, M., Sterky, F., Stromberg, S., Sundberg, M., Tegel, H., Tourle, S., Wahlund, E., Walden, A., Wan, J., Wernerus, H., Westberg, J., Wester, K., Wrethagen, U., Xu, L. L., Hober, S., Ponten, F. (2005) A human protein atlas for normal and cancer tissues based on antibody proteomics. *Mol. Cell. Proteomics* **4**, 1920-1932.
- Uhlen, M., Fagerberg, L., Hallstrom, B. M., Lindskog, C., Oksvold, P., Mardinoglu, A., Sivertsson, A., Kampf, C., Sjostedt, E., Asplund, A., Olsson, I., Edlund, K., Lundberg, E., Navani, S., Szgyarto, C. A., Odeberg, J., Djureinovic, D., Takanen, J. O., Hober, S., Alm, T., Edqvist, P. H., Berling, H., Tegel, H., Mulder, J., Rockberg, J., Nilsson, P., Schwenk, J. M., Hamsten, M., von Feilitzen, K., Forsberg, M., Persson, L., Johansson, F., Zwahlen, M., von Heijne, G., Nielsen, J., Ponten, F. (2015) Proteomics. Tissue-based map of the human proteome. *Science* **347**, 1260419.
- Uhlen, M., Zhang, C., Lee, S., Sjostedt, E., Fagerberg, L., Bidkhor, G., Benfeitas, R., Arif, M., Liu, Z., Edfors, F., Sanli, K., von Feilitzen, K., Oksvold, P., Lundberg, E., Hober, S., Nilsson, P., Mattsson, J., Schwenk, J. M., Brunnstrom, H., Glimelius, B., Sjoblom, T., Edqvist, P. H., Djureinovic, D., Micke, P., Lindskog, C., Mardinoglu, A., Ponten, F. (2017) A pathology atlas of the human cancer transcriptome. *Science* **357**. 10.1126/science.aan2507
- Wiederhold, T., Lee, M. F., James, M., Neujahr, R., Smith, N., Murthy, A., Hartwig, J., Gusella, J. F., Ramesh, V. (2004) Magicin, a novel cytoskeletal protein associates with the NF2 tumor suppressor merlin and Grb2. *Oncogene* **23**, 8815-8825.
- Yin, J. W., Wang, G. (2014) The Mediator complex: a master coordinator of transcription and cell lineage development. *Development* **141**, 977-987.